Materials Science in Semiconductor Processing 31 (2015) 551–560

Contents lists available at ScienceDirect

Materials Science in Semiconductor Processing

journal homepage: www.elsevier.com/locate/mssp

Electrochromic properties of electrochemically synthesized porphyrin/3-substituted polythiophene copolymers

Sadik Cogal [a,b], Melek Kiristi [b], Kasim Ocakoglu [c,d], Lutfi Oksuz [e], Aysegul Uygun Oksuz [b,*]

[a] Mehmet Akif Ersoy University, Faculty of Arts and Science, Department of Chemistry, 15030 Burdur, Turkey
[b] Suleyman Demirel University, Faculty of Arts and Science, Department of Chemistry, 32260 Isparta, Turkey
[c] Advanced Technology Research & Application Center, Mersin University, Ciftlikkoy Campus, TR-33343 Yenisehir, Mersin, Turkey
[d] Department of Energy Systems Engineering, Faculty of Technology, Mersin University, TR-33480 Tarsus, Mersin, Turkey
[e] Suleyman Demirel University, Faculty of Arts and Science, Department of Physics, 32260 Isparta, Turkey

ARTICLE INFO

Available online 12 January 2015

Keywords:
Porphyrin
3-Methylthiophene
3-Hexylthiophene
Electrochemical polymerization
Electrochromic

ABSTRACT

Porphyrins bearing 2-thienyl substituent were copolymerized with 3-methylthiophene and 3-hexylthiophene by using an electrochemical polymerization method in a tetrabutylammonium hexafluorophosphate/dichloromethane (TBAPF6/DCM) solution. The copolymers were examined with FT-IR, UV–vis spectrometer and cyclic voltammetry analyses. Electrochromic properties of the electrodeposited copolymers were investigated and a rapid and persistent coloration process based on redox reactions of the films was observed. The pale yellow color of thin films switched to gray when anodic potential was applied. Optical contrast at 600 nm was recorded by a spectrophotometer of the solid state devices and their durability was tested by chronoamperometric measurements during 1000 cycles.

1. Introduction

Electrochromic (EC) devices change their optical properties reversibly and persistently under applied DC voltages and have found applications, such as smart windows, optical displays and rear-view mirror [1,2]. A variety of materials such as transition metal oxides (TMOs) and polymers have been studied intensively for last decades to obtain electrically color changing EC devices [3,4]. Compared to TMOs, polymeric materials show superior EC performance because of their multicoloration effect and rapid response time to the applied voltage [5–7]. Moreover, the higher molar absorption potential of the polymers increases the coloration efficiencies of EC devices compared to inorganics [8,9]. Composite polymers [10–13] and copolymers [14–17] were studied in order to further improve EC properties.

Porphyrins have excellent electronic and optical properties because of their large π-electron conjugation system [18,19]. However, EC applications of porphyrin based materials are very limited and need further studies. For instance, electropolymerized triphenylamine substituted porphyrins showed multicolor EC characteristics in a liquid electrolyte medium [20]. In this approach, polythiophene derivatives can be used to improve the EC properties of porphyrins [21–23]. There are many methods to synthesize new conducting materials based polythiophene [24,25]. One of the most convenient methods among them is the direct copolymerization of thiophene monomer with conducting monomers by using either chemical or electrochemical process [26,27]. Electrochemical route is coming forward since it enables easy and fast film forming onto surface of various electrodes [25]. Electrochemical synthesis of thiophene copolymers with various monomers has been reported [28–30]. On the other

* Corresponding author. Tel.: +90 2462114082.
E-mail address: ayseguluygun@sdu.edu.tr (A.U. Oksuz).

http://dx.doi.org/10.1016/j.mssp.2014.12.036
1369-8001/

hand, there are only a few studies exist on the co-polymerization of thiophene and porphyrin derivatives. Copolymerizations of bithiophene and porphyrin, bearing thiophene moiety, have been studied recently [31–35]. It was shown that electrochemically synthesized copolymer film of 5,10,15,20-tetra(3-hienyl)porphyrin (TThP) and bithiophene (BiTh) exhibited good efficiency for solar cell application [34]. As another derivate, the alkyl side chain length of alkylthiophene types also provide appropriate molecular structure as well as good electrical and optical properties for the compositions [36,37].

In the present study, four types of copolymers were synthesized by 3-alkylthiophene derivatives (3-methylthiophene and 3-hexylthiophene) and porphyrin monomers (mezo-tetrakis(2-thienyl)porphyrin and mezo-tetrakis(2-thienyl)porphyrin zinc(II)) by using the anodic electrochemical polymerization in the tetrabutylammonium hexafluorophosphate/dichloromethane (TBAPF6/DCM) electrolyte. Currently, the molecular effect of the alkyl side chain in copolymer structures and their EC properties was investigated by potentiometric and spectrophotometric measurements.

2. Experimental

2.1. Materials

3-Methylthiophene (Aldrich, 98%), 3-hexylthiophene (Aldrich, ≥99%), dichloromethane (DCM, ≥%99,5), lithium perchlorate ($LiClO_4$), propylene carbonate (PC), polymethylmetacrylate (PMMA), and acetonitrile (ACN) were purchased from Sigma-Aldrich. Tetrabutylammonium hexafluorophosphate (TBAPF6) was purchased from Alfa-Aesar. All the materials were used as received. Meso-tetrakis(2-thienyl)porphyrin (Por) and meso-tetrakis(2-thienyl)porphyrin zinc(II) were synthesized as described in the literature [38,39].

2.2. General method for preparation of porphyrin/polythiophene copolymers

The porphyrin/polythiophene copolymer films were synthesized by using the electrochemical polymerization method. The experiments were carried out in a typical three electrodes cell in which a glass sheet with deposited indium-tin-oxide (ITO) was used as the working electrode, a platinum wire was used as the counter electrode and an Ag/AgCl electrode was used as the reference electrode. The ITO was cleaned ultrasonically in ethanol and then in DCM before use. The electrochemical experiments were performed with a Gamry PCl4/300 potentiostat/galvanostat. The chemical structures of porphyrin and thiophene monomers are shown in Fig. 1.

A DCM solution containing 2.5 mM Por, 15 mM 3-MT and 0.1 M TBAPF6 was prepared for polymerization. The potential applied to the working electrode was scanned between 0 and +2 V at scan rate of 25 mV s^{-1}. The ITO working electrode was removed from the solution, rinsed thoroughly with the DCM to remove the soluble monomer and oligomers on the film and finally dried in the air to obtain Por/3MT film. The other copolymer films of ZnPor/3MT, Por/3HT, and ZnPor/3HT were fabricated in the same way. The homopolymers of Por,

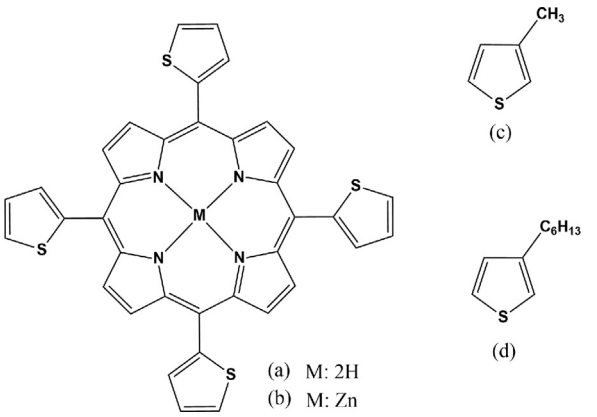

Fig. 1. The chemical structure of porphyrin (a), zinc porphyrin (b), 3-methlthiohene (c) and 3-hexythiophene (d) monomers.

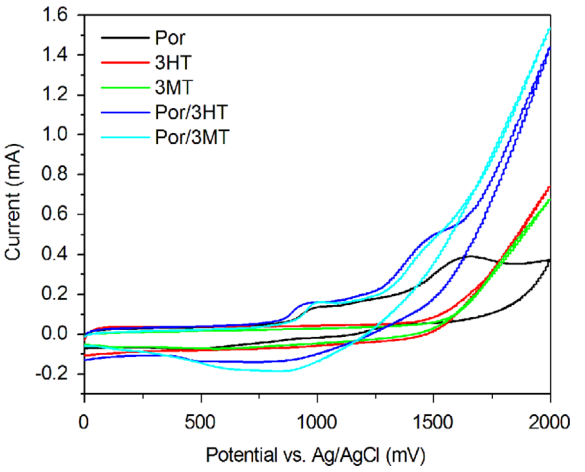

Fig. 2. The CVs of Por, 3HT, 3MT, Por/P3HT and Por/3MT in DCM solution containing 0.1 M TBAPF6. Working electrode: ITO, scan rate: 25 mV s^{-1}.

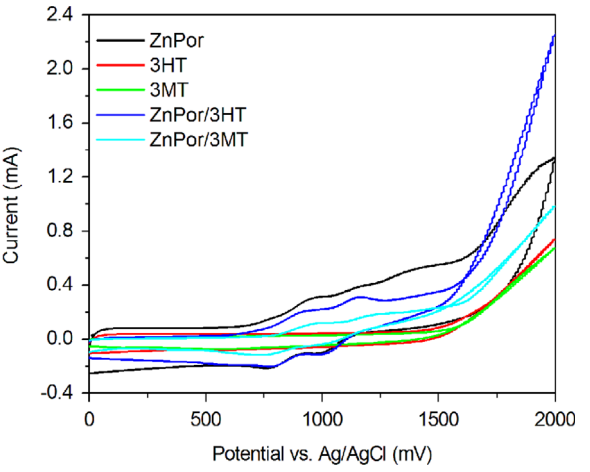

Fig. 3. The CVs of ZnPor, 3HT, 3MT, ZnPor/P3HT and ZnPor/3MT in DCM solution containing 0.1 M TBAPF6. Working electrode: ITO, scan rate: 25 mV s^{-1}.

ZnPor, 3HT and 3MT were obtained in electrolyte solution containing 2.5 mM of monomers, respectively.

2.3. Electrochromic device assembly

The transparent ion conductive gel electrolyte was prepared as described in the literature [2,8] and $LiClO_4$, PC, PMMA and ACN were used at the wt% of 3:7:70:20, respectively. The gel electrolyte was drop cast onto the electrochemically coated ITO coated glass electrode surface, the thickness was 1 μm. Then a second ITO coated glass layer was sandwiched as the counter electrode layer. Finally four edges of the devices were sealed with silicon sealant. The effective area of the devices was 4 cm^2.

Table 1
The oxidation onset potentials of monomers and copolymers.

	E_{ox}^{on} (mV, vs. Ag/AgCl)			
Por	898	1138	1379	–
ZnPor	829	1050	1237	1645
Por/P3MT	886	1311	1647	–
Por/P3HT	842	1285	1660	–
ZnPor/P3MT	790	1091	1608	–
ZnPor/P3HT	771	1050	1611	–

2.4. Characterization

FTIR spectra of copolymers were measured between 400 and 4000 cm^{-1} using Perkin-Elmer Spectrum BX FTIR system (Beaconsfield, Buckinghamshire, HP91QA, England). The NMR (400 MHz) spectra were recorded using a Bruker Ultrashield Plus Biospin GmbH spectrometer in CDCl3. The absorption spectra were recorded using Perkin-Elmer Lambda 20 UV–vis spectrometer. Scanning electron microscopy (SEM) images were taken with Philips XL-30S FEG scanning electron microscopy. Optical transmittance spectra of solid state EC devices were measured using a spectrophotometer (Ocean optics HR 4000, Mikropack Halogen Light Source HL-2000-FHSA in the 200–1000 nm wavelength range) combining with the potentiostat (Gamry PCI4/300 model) by sweeping potential between −1.5 V and +1.5 V and the scan rate was 50 mV s^{-1}. In addition, chronamperometric measurements of the solid state devices were carried out with the same potentiostat for stability testing.

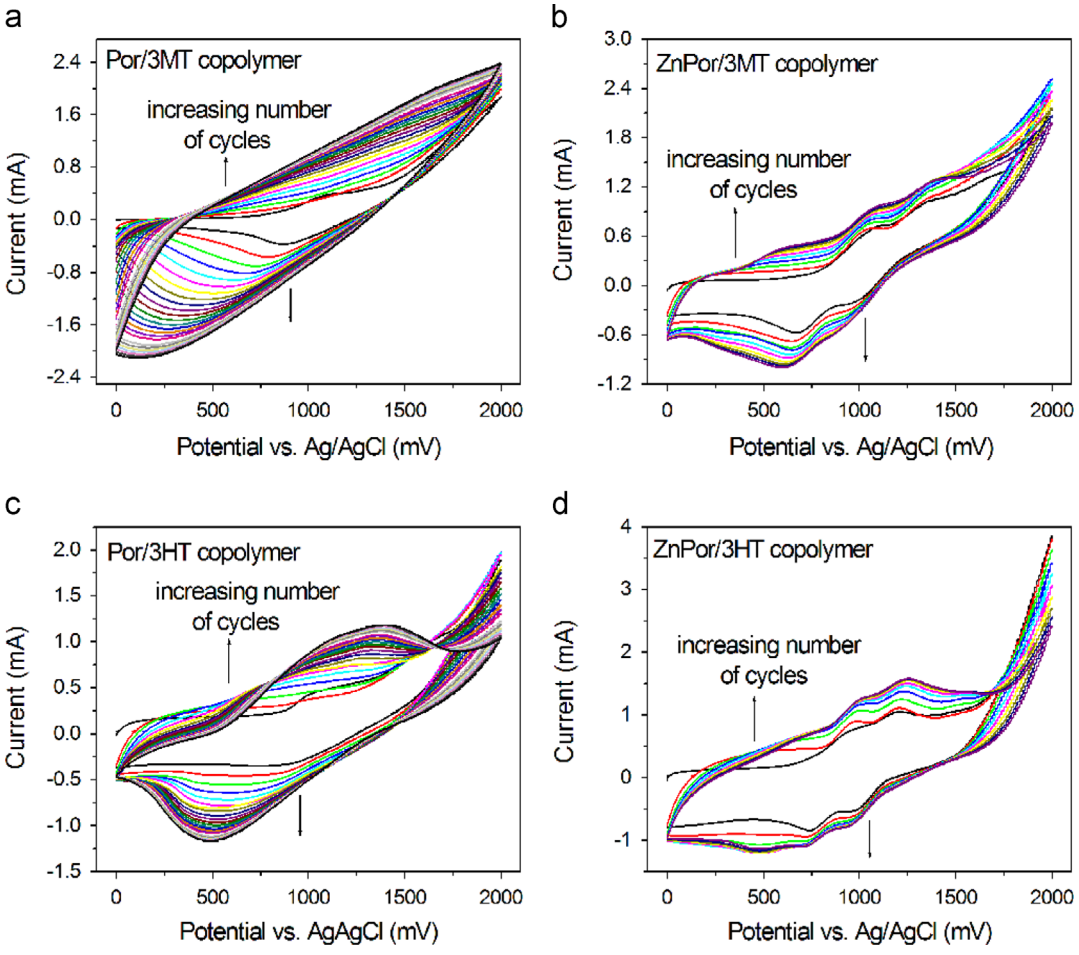

Fig. 4. The CVs of copolymers recorded on an ITO electrode in 0.1 M TBAPF6+DCM electrolyte solution containing 2.5 mM porphyrin and 15 mM thiophene, 25 mV s^{-1} potential scan rate.

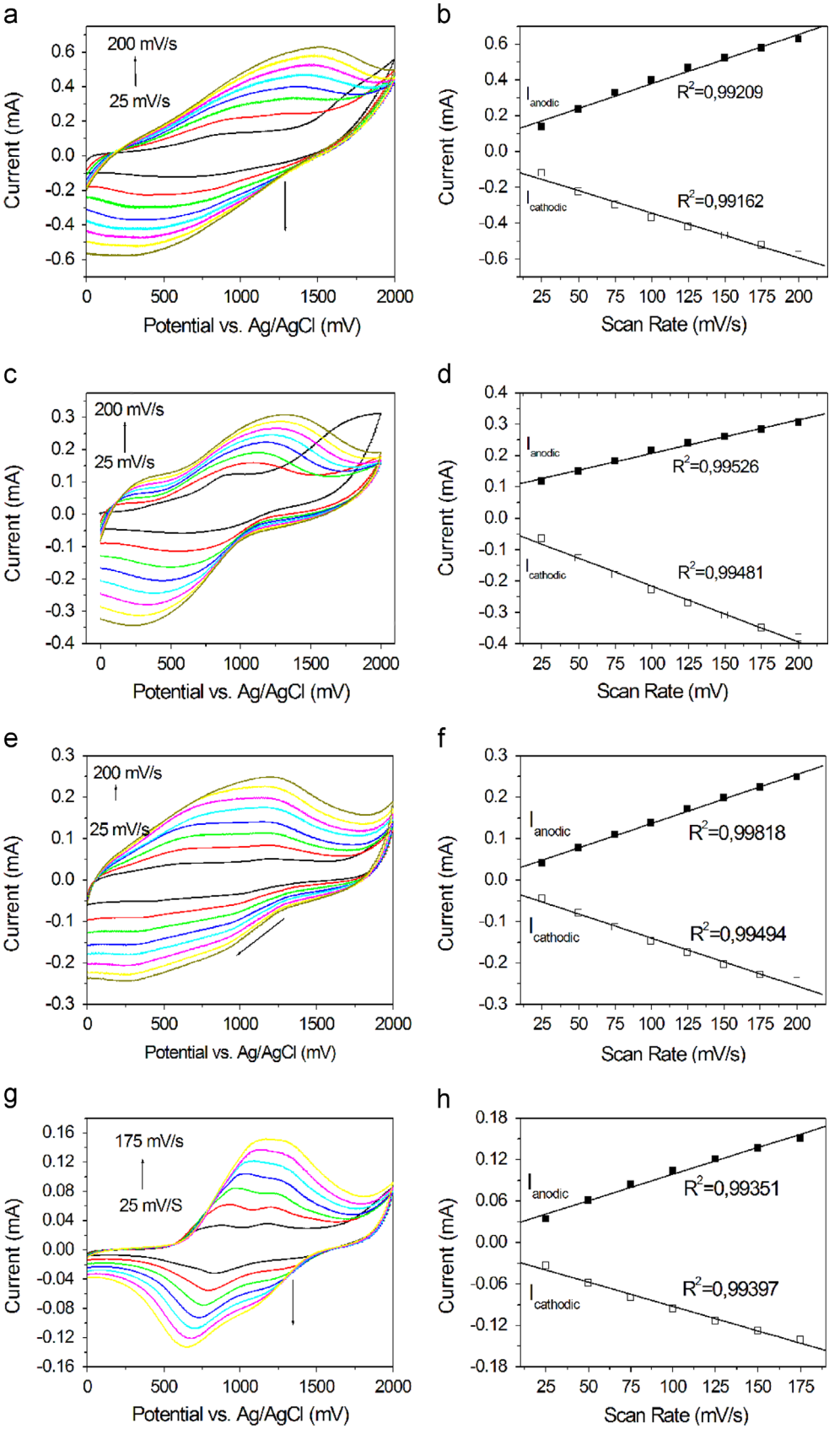

Fig. 5. Cyclic voltammograms and anodic–cathodic currents at different scan rates of Por/P3MT (a and b), Por/P3HT (c and d), ZnPor/P3MT (e and f) and ZnPor/P3HT (g and h) copolymer films in monomer free DCM solution containing TBAPF6 as electrolyte.

3. Results and discussion

3.1. Electrochemical studies

The electrochemical properties of monomers and copolymers were investigated by cyclic voltammetry in DCM solution containing TBAPF6 as electrolyte using ITO working electrode. Figs. 2 and 3 show the first anodic scan of monomers and copolymers. For comparison, the cyclic voltammograms (CVs) of Por, ZnPor, 3MT and 3HT were also shown in Figs. 2 and 3. Por has three oxidation waves while ZnPor has four oxidation waves. The first and the second oxidation waves of both porphyrins are reversible. The third oxidation wave of ZnPor was quasi-reversible and the third oxidation wave of Por and the fourth oxidation wave of ZnPor were irreversible. Bhyrappa and Bhavana reported the electrochemical properties of meso-tetrathieyl porphyrins and found two reversible oxidation waves by anodic scanning from 0.0 to 1.2 V in DCM solution containing 0.1 M tetrabutylammonium hexafluorophosphate (TBAHFP) as an electrolyte [39]. In this study, as can be seen from the cyclic voltammograms all scans were carried out in the potential range of 0.0–2.0 V. So, the differences in the number of oxidation waves were obtained by changing the electrochemical conditions. Copolymers show three oxidation waves in the first anodic scan. The oxidation potential over 1600 mV is related to the thiophene monomers. Furthermore, the substitution of the two H central atoms in Por by Zn(II) lowers the first oxidation potential of ZnPor and its copolymers. The oxidation onset potentials of monomers and copolymers are summarized in Table 1.

Fig. 4 shows a series of CVs recorded for each copolymer on ITO working electrode in DCM solution containing TBAPF6 as an electrolyte. To minimize the degradation of copolymer films on the electrode surface, the copolymerization process were recorded at the anodic potential. All of the depositions of copolymers were carried out in the same potential range from 0 to 2.0 V. With increasing the number of cycle, a new oxidation peak was observed and the intensity of the oxidation and reduction current was increased, indicating the formation of copolymers on the electrode surface. Chen et al. reported the electrochemical polymerization of Por and found that the increase of oxidation current above +1.2 V with the increase of scanning cycles can be attributed to the oxidation of meso-2-thienyl groups of porphyrin macrocycle [40]. 3MT and 3HT monomers were electrochemically polymerized by Pang et al. [41]. Compared with those studies of homopolymers of Por and 3-substituted thiophene monomers [33,34], the CVs of Por/3MT, ZnPor/3MT, Por/3HT and ZnPor/3HT copolymers are different than those of homopolymers. These results also have confirmed the formation of the copolymers. The oxidation potentials of Por/3MT, ZnPor/3MT, Por/3HT and ZnPor/3HT have started at about 886, 790, 842, and 771 mV (vs. Ag/AgCl), respectively, during the first potential range. The polymer films formed on the electrode were oxidized easier than monomer, therefore, the oxidation potentials of copolymers shifted to less positive potentials from the second cycle [42]. In addition, it might be concluded from these results that the copolymers could be formed in random structures. In general, electropolymerization of two different conjugated monomers have been resulted in a random copolymer [43,44].

The results obtained above strongly suggest that the electrochemical oxidation of the thiophene and porphyrin monomers give the formation of their corresponding copolymer films on the electrode surface. At this point, the absorption of copolymer films on the electrode surface and their electrochemical response were investigated. Once the ITO electrodes were coated with the copolymers as described above, they were immersed into the

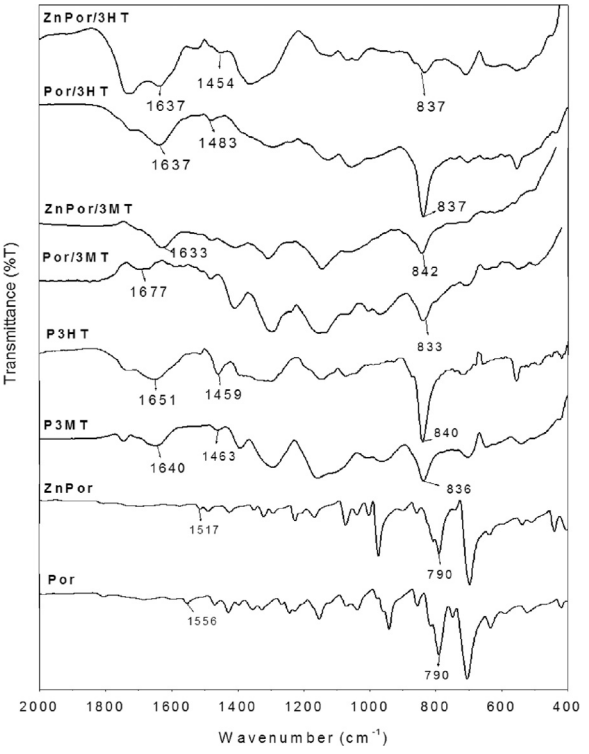

Fig. 6. FT-IR spectra of the polymer and copolymers.

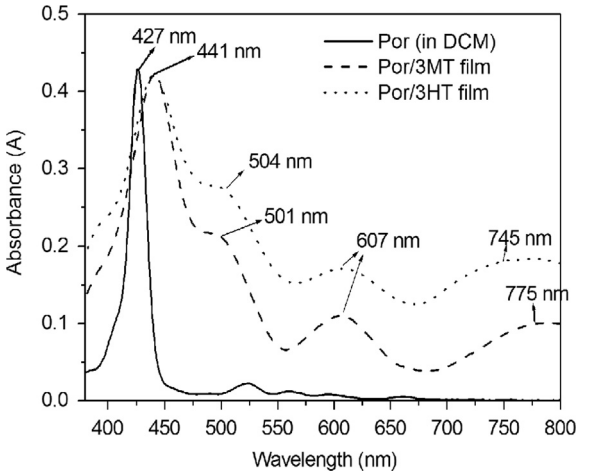

Fig. 7. UV–vis absorption spectra of Por and Por/3MT and Por/3HT films.

monomer free electrolyte solution. Fig. 5 presents the CVs of copolymer films recorded with different scan rate (from 25 mV s^{-1} to 200 mV s^{-1}) and the anodic–cathodic peak currents which plotted to the scan rate. Both anodic and cathodic peak currents for all copolymers increase linearly with increasing the scan rate indicating the copolymer films are well adsorbed on the working electrode surface [45].

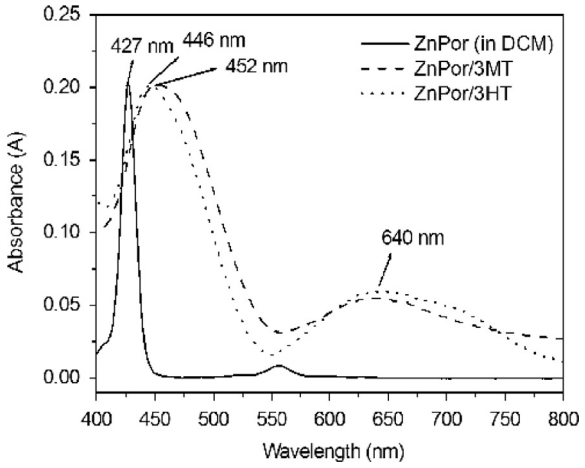

Fig. 8. UV–vis absorption spectra of ZnPor and ZnPor/3MT and ZnPor/3HT films.

Diffusion coefficient '*D*' was determined using Randles–Sevcik equation [46]

$$i_p = 268,600 n^{3/2} A D^{1/2} C v^{1/2} \quad (1)$$

Table 2
Oxidation potentials, thicknesses and light transmittance changes of copolymer films.

Copolymer	Oxidation potential $LiClO_4$/PC (1 mol dm^{-3}) electrolyte (mV)	Thickness of copolymer films deposited on ITO (nm)	Light transmittance changes (ΔT%) at 600 nm
Por/3MT	563	1090	21.02
ZnPor/3MT	724	73	9.49
Por/3HT	686	1380	29.18
ZnPor/3HT	799	437	11.49

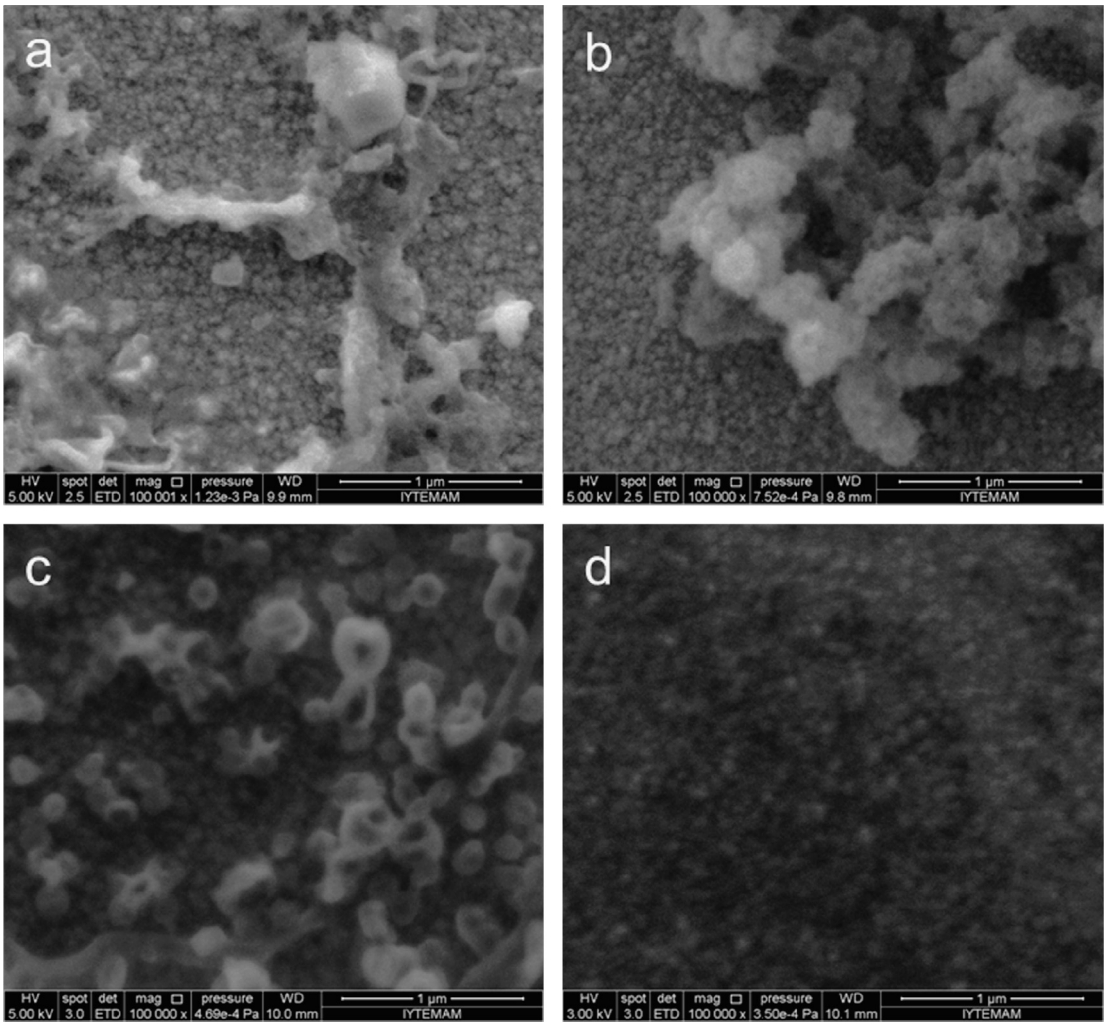

Fig. 9. SEM images of (a) Por/3MT, (b) Por/3HT, (c) ZnPor/3MT, and (d) ZnPor/3HT deposited on ITO.

where i_p is the peak current, v is scan rate in V s^{-1} (0.05 V s^{-1}), A is area of film in cm^2 (1 cm^2 in this work), C is the bulk concentration (17.5 mM), and n is number of electron transfer per molecule in oxidation process (here $n=1$). Using these values, the diffusion coefficient was calculated to be 5.11×10^{-8}, 2.03×10^{-8}, 0.55×10^{-8} and 0.34×10^{-8} cm^2 s^{-1} for Por/3MT, ZnPor/3MT, Por/3HT and ZnPor/3HT copolymers, respectively.

3.2. Absorption studies

Fig. 6 shows the FT-IR spectra of polymers and copolymers. To obtain a sufficient amount of copolymer for characterization, ITO electrode was used as a working electrode and a series of CVs was applied. According to the spectrum of Por and ZnPor, the bands at 1517 and 1556 cm^{-1} originate from the C=C vibrations of the aromatic system and the bands around 790 cm^{-1} are related to the deformation vibrations of aromatic rings. The bands at 820 and 819 cm^{-1} are assigned to the C–S stretching of Por and ZnPor, respectively. In the spectrum of P3MT and P3HT, the bands at 1640 and 1651 cm^{-1} are assigned to the C=C stretching mode and the bands at 1463 and 1459 cm^{-1} are related to the corresponding aromatic mode, respectively [47]. The characteristic C–S stretching peaks of P3MT, P3HT, Por/3MT, ZnPor/3MT, Por/3HT and ZnPor/3HT were observed at 836, 840, 839, 842, 837 and 837 cm^{-1}, respectively [42]. While Por/3MT copolymer shows aromatic C=C stretching at 1677 cm^{-1}, the ZnPor/3MT copolymer shows the same stretching peak at 1633 cm^{-1}. In the spectrum of Por/3HT copolymer, aromatic C=C peak was observed 1637 cm^{-1} and corresponding aromatic ring mode appeared at 1483 cm^{-1}. FT-IR spectrum of ZnPor/3HT copolymer shows aromatic C=C peak at 1637 cm^{-1} and corresponding aromatic ring mode appears at 1454 cm^{-1}. All of copolymers show C–H deformation vibrations around 710 cm^{-1}.The similar stretching modes of homopolymers and copolymers result in overlapping of the absorption peaks. Nevertheless, both differences in the characteristic peaks of thiophene unit and electrochemical results indicate the copolymer formation.

Fig. 7 presents the UV–vis absorption spectrum of Por in DCM solution and Por/3MT and Por/3HT copolymer films on ITO electrode. Copolymerization of Por with 3-alkylthiophene derivatives shifted the absorption from 427 to 441 nm. In addition, new absorption bands were observed between 450 and 800 nm. The UV–vis absorption spectra of ZnPor in DCM solution and ZnPor/3MT and ZnPor/3HT copolymer films on ITO electrode are shown in Fig. 8. Copolymerization of ZnPor with 3-alkylthiophene derivatives shifted the absorption band from 427 nm to 441 nm for ZnPor/3MT and 452 nm for ZnPor/3HT. This shift in the absorption bands is attributed to the extension in the conjugation of porphyrin macrocycle with respect to thiophene units in copolymer structure. The absorption bands between 400 and 450 nm are due to the π–π^* transitions known as Soret band of the macrocycle of

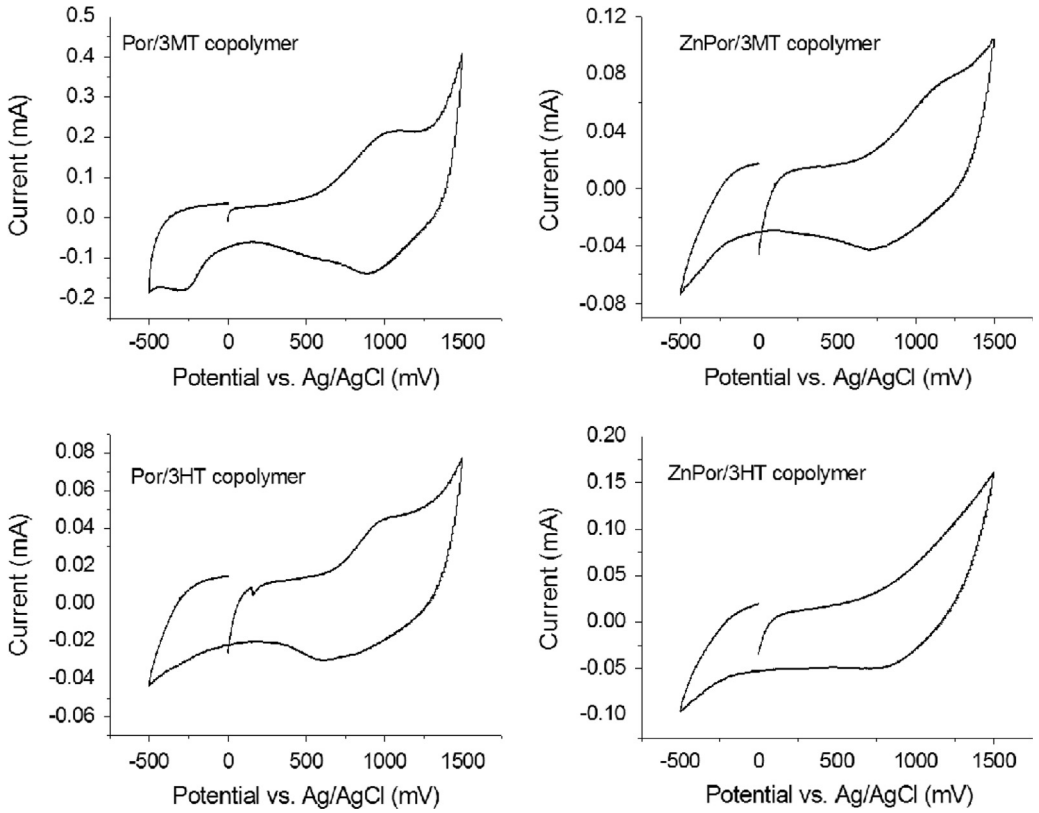

Fig. 10. Cyclic voltammograms of the copolymers electrodes measured in $LiClO_4$/PC (1 mol dm^{-3}) electrolyte and a Pt was used as the counter electrode, and an Ag/AgCl served as reference electrode. The scan rate is 50 mV s^{-1}.

porphyrin. P3MT and P3HT polymer films have a broad absorption band between 350 and 650 nm [48,49].

3.3. Electrochromic properties

Morphological properties are very important for electroactivity and the optical variations of the EC materials. The SEM images (Fig. 9) illustrate the surface structure of the thin films deposited at the same conditions. Generally, globular structure revealed on the thin film surface, but ZnPor copolymers showed more compact coating tendency. Surface roughness provides interpenetrating pathways for ions under applied voltages [50]. The thickness of the copolymer films on ITO electrode can be controlled by changing the number of the cycle up to oxidation current values become constant. Interestingly, the thickness of the copolymer films showed diversity after five cycles deposition, as a result of the different electroactivity (Table 2). It can be concluded that metal center of porphyrin affected the electopolymerization process and resulted lower deposition at the same conditions [51]. As thickness increases, the maximum change in optical transmittance ($\Delta T = T_{\text{bleached}} - T_{\text{coloured}}$) increases due to the increasing charge capacity depending on the active sites of the film under applied voltages [50]. This shows similarity with the results (Table 2).

In order to determine of redox potentials of the copolymers, CV studies were performed. The oxidation peak potentials of the films are Por/3MT (563) < Por/3HT (686) < Zn/Por/3MT (724) < Zn/Por/3HT (799 mV vs. Ag/AgCl) indicating that Por/3MT is easier to oxidize and switch its color (Fig. 10). It exhibits also better π-conjugation, which corroborates the introduction of thiophene unit into the porphyrin-based polymer main chain [52]. Decreasing oxidation potential originated from π-conjugation can enhance EC stability of the prepared film [53,54]. This phenomenon is also confirmed by chronoamperometric measurements. It

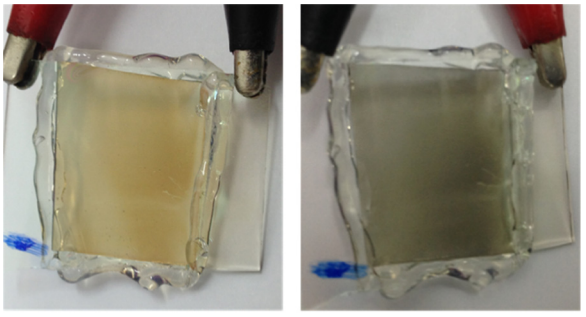

Fig. 12. Photographs images of Por/3MT copolymer film deposited on ITO electrode at two different applied potentials.

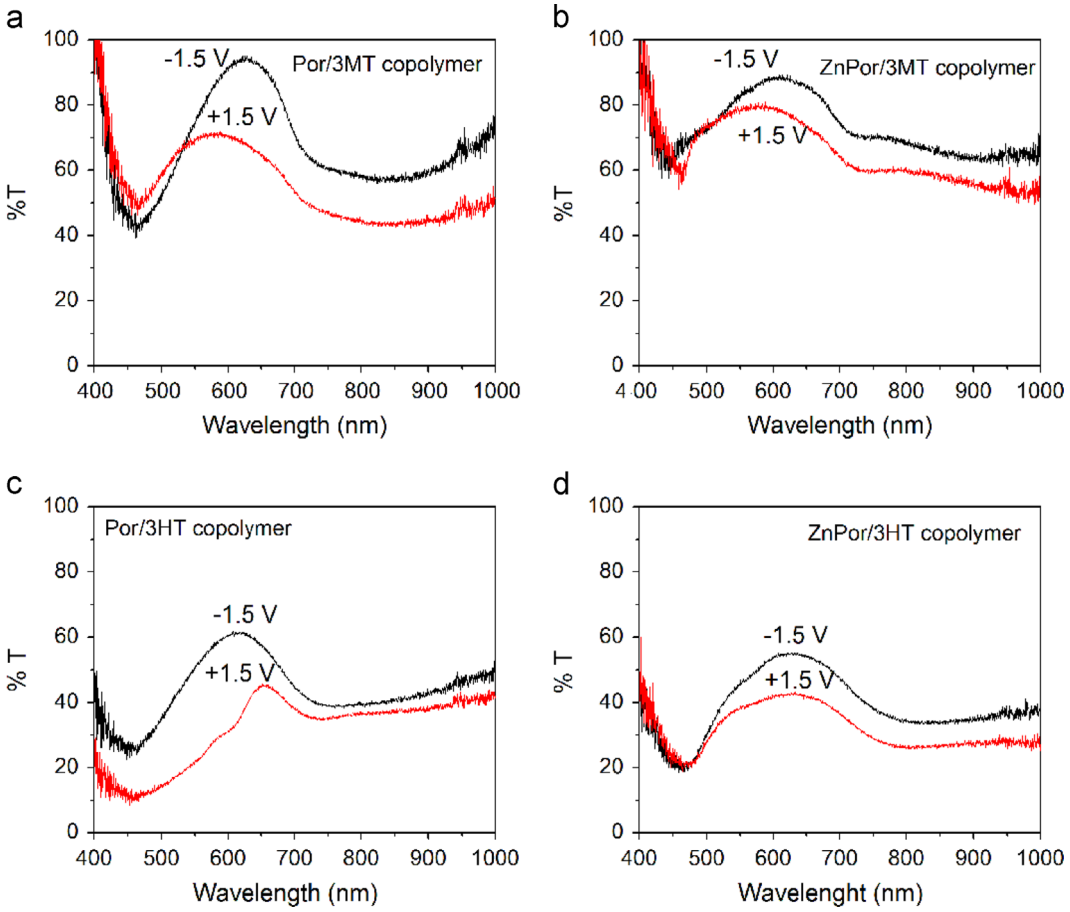

Fig. 11. Optical measurements of the solid state devices.

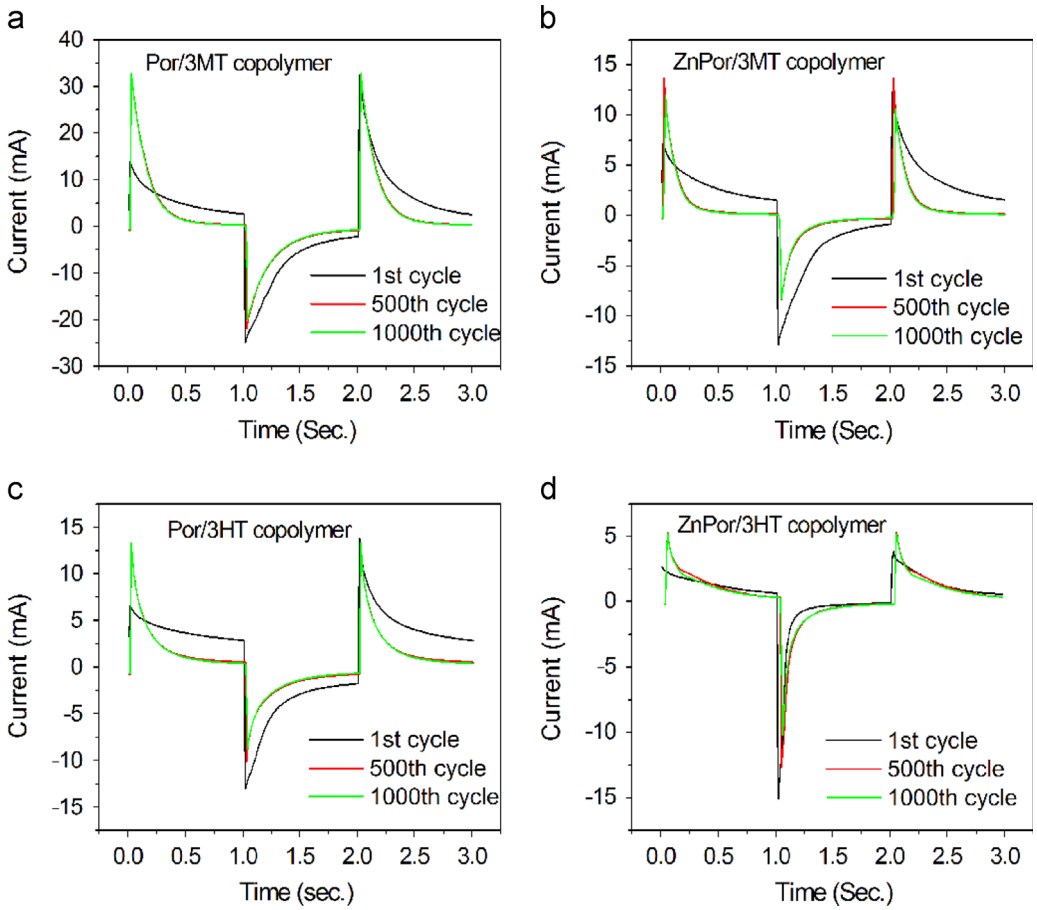

Fig. 13. Chronamperometric measurements of the solid state devices.

was reported that the planarity and S–S interaction of alkylthiophenes promote highly ordered π-stacked structures and high hole mobilities [55]. Shorter molecular chain of Por/3MT enables to reduce steric hindrance, extend conjugation, enhance absorption, and improve charge transport property. Thus Por/3MT showed better EC performance.

Zinc porphyrin ring of the polymers play an important role in solubilizing, induce self-assembly, and enhance molecular ordering. However in copolymer structures increased oxidation potential and reduced EC activity. Fig. 11 shows maximum transmittance (%*T*) curves of the solid state EC devices. In the neutral (0 V) and reduced state the devices are yellow pale/transparent, during the p-doping process color switching to gray (Fig. 12). As shown in the figures, the transmittance of the EC devices is lower at anodic potential and higher when cathodic potential applied. The EC devices' light transmittance changes ($\Delta T\%$) in the visible region are Por/3HT (29.18) > Por/3MT (21.02) > ZnPor/3HT(11.49) ZnPor/3MT (9.49 at 600 nm) showing notable values (Table 2). As mentioned above, lower oxidation potentials and higher thickness values of the thin films of both Por/3MT and Por/3HT, resulted in higher $\Delta T\%$ under applied voltage.

Chronamperometric characterization was used to test the stability and repeatability of the devices during 1000 cycles. Li et al. also were used this method and followed current curves of a complementary EC device, they figured out that after 150,000 cycles current values remained the same as the beginning [56]. In this study, Fig. 13 shows the current response of the solid-state EC devices against to applied cyclic potential of $\pm$ 1.5 V with the time interval set to 0.01 s. The switching time of the devices (area of 4 cm^2) was less than one second when $-$1.5 V was applied and one second when $+$1.5 V was applied. It can be seen that Por/3MT showed more stable activity and color changes during cycles, unlike others. In the copolymer structures electronic delocalization and amount of charge transferred from the porphyrin or zinc/porphyrin donor moiety to the conjugated alkylthiophene side chain acceptor moiety leads to the formation of electron–hole pairs and improves the electrons movement and transition [19,57].

4. Conclusions

Novel copolymers based on porphyrin–thiophene units were synthesized by using electrochemical polymerization and characterized by spectroscopic and electrochemical methods. The spectroscopic results indicate that the copolymers show red-shifted absorptions. Oxidation onset potentials of the copolymer films were determined by cyclic voltammetry in PC containing $LiClO_4$ for EC application. It was figured out that lower oxidation state of thin

films of both Por/3MT and Por/3HT copolymers showed higher stability and better optical properties as solid-state EC device applications.

Acknowledgments

This work was supported financially by the grant of Suleyman Demirel University, Scientific Research Projects (2950-D-11). The authors also thank to Plus Plasma Research Lab.

References

[1] M. Kiristi, F. Bozduman, A. Uygun Oksuz, O. Oksuz, A. Hala, Ind. Eng. Chem. Res. 53 (2014) 15917–15922.
[2] M. Kiristi, F. Bozduman, A. Gulec, E. Teke, A. Uygun Oksuz, O. Oksuz, H. Deligoz, J. Macromol. Sci. Pure Appl. Chem 51 (2014) 481–487.
[3] P.M. Beaujuge, C.M. Amb, J.R. Reynolds, Acc. Chem. Res. 43 (2010) 1396–1407.
[4] P.R. Somani, S. Radhakrishnan, Mater. Chem. Phys. 77 (2002) 117–133.
[5] A. Balan, D. Baran, L. Toppare, Polym. Chem. 2 (2011) 1029–1043.
[6] R. Mortimer, J. Electrochromic Mater. Annu. Rev. Mater. Res. 41 (2011) 241–268.
[7] C.M. Amb, A.L. Dyer, J.R. Reynolds, Chem. Mater. 23 (2011) 397–415.
[8] V.K. Thakur, G. Ding, J. Ma, P.S. Lee, X. Lu, Adv. Mater. 24 (2012) 4071–4096.
[9] A.T. Taskin, A. Balan, Y.A. Udum, L. Toppare, Smart Mater. Struct. 19 (2010) 065005.
[10] X.H. Xia, J.P. Tu, J. Zhang, X.H. Huang, X.L. Wang, W.K. Zhang, H. Huang, Electrochem. Commun. 11 (2009) 702–705.
[11] A.C. Sonavane, A.I. Inamdar, H.P. Deshmukh, P.S. Patil, J. Phys. D: Appl. Phys. 43 (2010) 315102.
[12] C. Sonavane, A.I. Inamdar, D.S. Dalavi, H.P. Deshmukh, P.S. Patil, Electrochim. Acta 55 (2010) 2344–2351.
[13] S. Bhandari, M. Deepa, S.N. Sharma, A.G. Joshi, A.K. Srivastava, R. Kant, J. Phys. Chem. C 114 (2010) 14606–14613.
[14] S. Xiong, Y. Xiao, J. Ma, L. Zhang, X. Lu, Macromol. Rapid Commun. 28 (2007) 281–285.
[15] S. Xiong, P. Jia, K.Y. Myab, J. Ma, F. Boey, X. Lu, Electrochim. Acta 53 (2008) 3523–3530.
[16] M. Ak, B. Gacal, B. Kiskan, Y. Yagci, L. Toppare, Polymer 49 (2008) 2202–2210.
[17] A.P. Saxena, M. Deepa, A.G. Joshi, S. Bhandari, A.K. Srivastava, ACS Appl. Mater. Interfaces 3 (2011) 1115–1126.
[18] H. Zhang, X. Zheng, H. Li, B. Jin, C. Wang, Y. Shen, J. Hua, J. Photochem. Photobiol. A: Chem. 272 (2013) 58–64.
[19] J. Durantini, G.M. Morales, M. Santo, M. Funes, E.N. Durantini, F. Fungo, T. Dittrich, L. Otero, M. Gervaldo, Org. Electron. 13 (2012) 604–614.
[20] M. Gervaldo, M. Funes, J. Durantini, L. Fernandez, F. Fungo, L. Otero, Electrochim. Acta 55 (2010) 1948–1957.
[21] E. Costa Rios, A.V. Rosario, A.F. Nogueira, L. Micaroni, Sol. Energy Mater. Sol. Cells 94 (2010) 1338–1345.
[22] Y. Pang, X. Li, H. Ding, G. Shi, L. Jin, Electrochim. Acta 52 (2007) 6172–6177.
[23] A. Lakshmi, R.J. Anandha, G. Gopu, P. Arumugam, C. Vedhi, Electrochim. Acta 92 (2013) 452–459.
[24] H. Guo, L. Liu, H. Shu, X. Yang, Z. Yang, M. Zhou, J. Tan, Z. Yan, H. Hu, X. Wang, J. Power Sources 247 (2014) 117–126.
[25] K. Furuta, H. Koyama, S. Honma, K. Nakabayashi, M. Atobe, Electrochemistry 81 (2013) 334–336.
[26] B. Qu, Z. Jiang, Z. Chen, L. Xiao, D. Tian, C. Gao, W. Wei, Q. Gong, J. Appl. Polym. Sci. 124 (2012) 1186–1192.
[27] B. Ustamehmetoglu, F. Demir, E. Sezer, Prog. Org. Coat. 76 (2013) 1515–1521.
[28] B. Yue, C. Wang, P. Wagner, Y. Yang, X. Ding, D.L. Officer G.G. Wallace, Synth. Metals 162 (2012) 2216–2221.
[29] J. Gao, Y.-H. Lai, Polymer 50 (2009) 1830–1834.
[30] Y.-j. Tao, Y.-j. Zhou, X.-Q. Xu, Z.-Y. Zhang, H.-F. Cheng, W.-W. Zheng, Electrochim. Acta 78 (2012) 353–358.
[31] C. Paul-Roth, J. Rault-Berthelot, G. Simonneaux, J. Letessier, J-F. Bergamini, J. Electroanal. Chem. 606 (2007) 103–116.
[32] W. Chen, Y. Wang, C. Brückner, C.M. Li, Y. Lei, Sens. Actuators B: Chem. 147 (2010) 191–197.
[33] B. Ballarin, R. Seeber, L. Tassi, D. Tonelli, Synth. Metals 114 (2000) 279–285.
[34] K. Takechi, T. Shiga, T. Motohiro, T. Akiyama, S. Yamada, H. Nakayama, K. Kohama, Sol. Energy Mater. Sol. Cells 90 (2006) 1322–1330.
[35] K. Sugawa, T. Akiyama, S. Yamada, Thin Solid Films 516 (2008) 2502–2506.
[36] D.C. Bento, E.C.R. Maia, T.N.M. Cervantes, R.V. Fernandes, E. Di Mauro, E. Laureto, M.A.T. da Silva, J.L. Duarte, I.F.L. Dias, H. de Santana, Synth. Metals 162 (2012) 2433–2442.
[37] H.S. Lee, J.H. Cho, K. Cho, Y.D. Park, J. Phy. Chem. C 117 (2013) 11764–11769.
[38] B. Purushothaman, B. Varghese, P. Bhyrappa, Acta Crystallogr. Sec. C 57 (2001) 252–253.
[39] P. Bhyrappa, P. Bhavana, Chem. Phys. Lett. 349 (2001) 399–404.
[40] W. Chen, Y. Wang, C. Brückner, C.M. Li, Y. Lei, Sens. Actuators B 147 (2010) 191–197.
[41] Y. Pang, X. Li, H. Ding, G. Shi, L. Jin, Electrochim. Acta 52 (2007) 6172–6177.
[42] P. Kumar, K. Ranjith, S. Gupta, C. Ramamurthy, Electrochim. Acta 56 (2011) 8184–8191.
[43] T. Yohannes, J.C. Carlberg, O. Inganäs, T. Solomon, Synth. Metals 88 (1997) 15–21.
[44] W.J. Doherty, R.J. Wysocki, N.R. Armstrong, S.S. Saavedra, Macromolecules 39 (2006) 4418–4424.
[45] A. Uygun, Talanta 79 (2009) 194–198.
[46] A.J. Bard, L.R. Faulkner, Electrochemical Methods, second ed. Wiley-VCH, New York, 2001.
[47] Ö. Papila, L. Toppare, Y. Yagci, L. Cianga, Int. J. Polym. Anal. Charact. 9 (2004) 13–28.
[48] M.T. Khan, M. Bajpai, A. Kaur, S.K. Dhawan, S. Chand, Synth. Metals 160 (2010) 1530–1534.
[49] R. Valaski, S. Ayoub, L. Micaroni, I.A. Hümmelgen, J. Solid State Electrochem. 6 (2012) 231–236.
[50] K.-S. Ahn, Y.-C. Nah, Y.-E. Sung, J. Vac. Sci. Technol. A: Vac. Surf. Films 20 (4) (2002) 1468.
[51] V. Çakır, F. Demir, Z. Bıyıklıoğlu, A. Koca, H. Kantekin, Dyes Pigments 98 (3) (2013) 414–421.
[52] H. Zhan, S. Lamare, A. Ng, T. Kenny, H. Guernon, W.-K. Chan A.B. Djurišić, P.D. Harvey, W.-Y. Wong, Macromolecules 44 (13) (2011) 5155–5167.
[53] P. Karastatiris, J.A. Mikroyannidis, I.K. Spiliopoulos, J. Polym. Sci. A: Polym. Chem. 46 (2008) 2367–2378.
[54] X. Fu, C. Jia, S. Wu, X. Weng, J. Xie, L. Deng, Synth. Metals 188 (2014) 104–110.
[55] X. Huang, C. Zhu, S. Zhang, W. Li, Y. Guo, X. Zhan, Y. Liu, Z. Bo, Macromolecules 41 (2008) 6895–6902.
[56] M. Li, Y. Wei, J. Zheng, D. Zhu, C. Xu, Org. Electron. 15 (2014) 428–434.
[57] A.S. Shalabi, A.M. El Mahdy, H.O. Taha, J. Nanopart. Res. 15 (6) (2013) 1–16.